ИНСТИТУТ ЯДЕРНОЙ ФИЗИКИ СО АН СССР

S.E. Baru, M.V. Beilin, A.E. Blinov,
V.E. Blinov, A.E. Bondar, A.D. Bukin,
V.R. Groshev, S.G. Klimenko, G.M. Kolachev,
A.P. Onuchin, V.S. Panin, I.Ya. Protopopov,
A.G. Shamov, V.A. Sidorov, Yu.I. Skovpen,
A.N. Skrinsky, V.A. Tayursky, V.I. Telnov,
Yu.A. Tikhonov, G.M. Tumaikin, A.E. Undrus,
A.I. Vorobiov, V.N. Zilich

# MEASUREMENT OF THE BRANCHING RATIO FOR $\Upsilon(1S)$ STATE INTO $\mu^+\mu^-$ AND SEARCH FOR DECAYS $\Upsilon(1S) \to \pi^+\pi^-$, $K^+K^-$, $p\bar{p}$

PREPRINT 91-110

НОВОСИБИРСК

Measurement of the Branching Ratio
for $\Upsilon(1S)$ State into $\mu^+\mu^-$
and Search for Decays $\Upsilon(1S) \to \pi^+\pi^-, K^+K^-, p\bar{p}$

*S.E. Baru, M.V. Beilin, A.E. Blinov,*
*V.E. Blinov, A.E. Bondar, A.D. Bukin,*
*V.R. Groshev, S.G. Klimenko, G.M. Kolachev,*
*A.P. Onuchin, V.S. Panin, I.Ya. Protopopov,*
*A.G. Shamov, V.A. Sidorov, Yu.I. Skovpen,*
*A.N. Skrinsky, V.A. Tayursky, V.I. Telnov,*
*Yu.A.Tikhonov, G.M.Tumaikin, A.E.Undrus,*
*A.I. Vorobiov, V.N. Zilich*

Institute of Nuclear Physics
630090, Novosibirsk 90, USSR

ABSTRACT

In the experiment with $e^+e^-$-beams performed at the VEPP-4 storage ring with the MD-1 detector we have measured $B_{\mu\mu}$, the branching ratio for the decay of $\Upsilon(1S)$ state into $\mu^+\mu^-$. We obtain $B_{\mu\mu} = (2.12 + 0.20 + 0.10)\%$. It is shown that the continuum and resonance interference should be taken into account. For the first time the upper limits on the branching ratio for the decays $\Upsilon \to \pi^+\pi^-$, $K^+K^-$, $p\bar{p}$ have been obtained: $B_r(\Upsilon \to \pi^+\pi-) < 5 \cdot 10^{-4}$, $B_r(\Upsilon \to (K^+K^-) < 5 \cdot 10^{-4}$, $B_r(\Upsilon \to p\bar{p}) < 5 \cdot 10^{-4}$.



## INTRODUCTION

Recently many experiments measuring the $\Upsilon$ leptonic decays have been performed [1–10]. In this paper the result of a new measurement of the branching ratio for the decay $\Upsilon \to \mu^+\mu^-$ ($B_{\mu\mu}$) is presented. We also have measured the upper limits for the decays $\Upsilon \to \pi^+\pi^-$, $K^+K^-$, $p\bar{p}$ which hadn't been measured before. The experiment was carried out using the MD-1 detector at the VEPP-4 storage ring. We observed the production of the $\Upsilon$ in $e^+e^-$-collisions. Collinear and multihadron events were selected. A signal from the resonance in the $\mu^+\mu^-$-channel was observed as the small increase in muon yield at the resonance peak with respect to the quantum electrodynamic (QED) continuum. For the continuum subtraction the data collected in nonresonant region have been used. In order to determine $B_{\mu\mu}$ we first obtain $\bar{B}_{\mu\mu} = \sigma_r^\mu/\sigma_r^h$, where $\sigma_r^\mu$ and $\sigma_r^h$ are the total resonance cross sections for muons and hadrons respectively. When $e$-$\mu$-$\tau$ universality is assumed, we have

$$B_{\mu\mu} = \bar{B}_{\mu\mu}/(1 + 3\bar{B}_{\mu\mu}). \qquad (1)$$

Experimental data were taken during two runs, the total integrated luminosity is 20.4 pb$^{-1}$. During the first run 3.4 pb$^{-1}$ at the continuum and 5.1 pb$^{-1}$ in the resonance were collected. At the second run the energy range scanning was performed in a mass region $\sqrt{s} = 7.6 \div 10$ GeV.

## 1. EXPERIMENTAL APPARATUS

The layout of the MD-1 detector is shown in Fig. 1. Charged particles are detected by 38 **proportional** chambers covered a solid angle of $0.8 \times 4\pi$ sr.

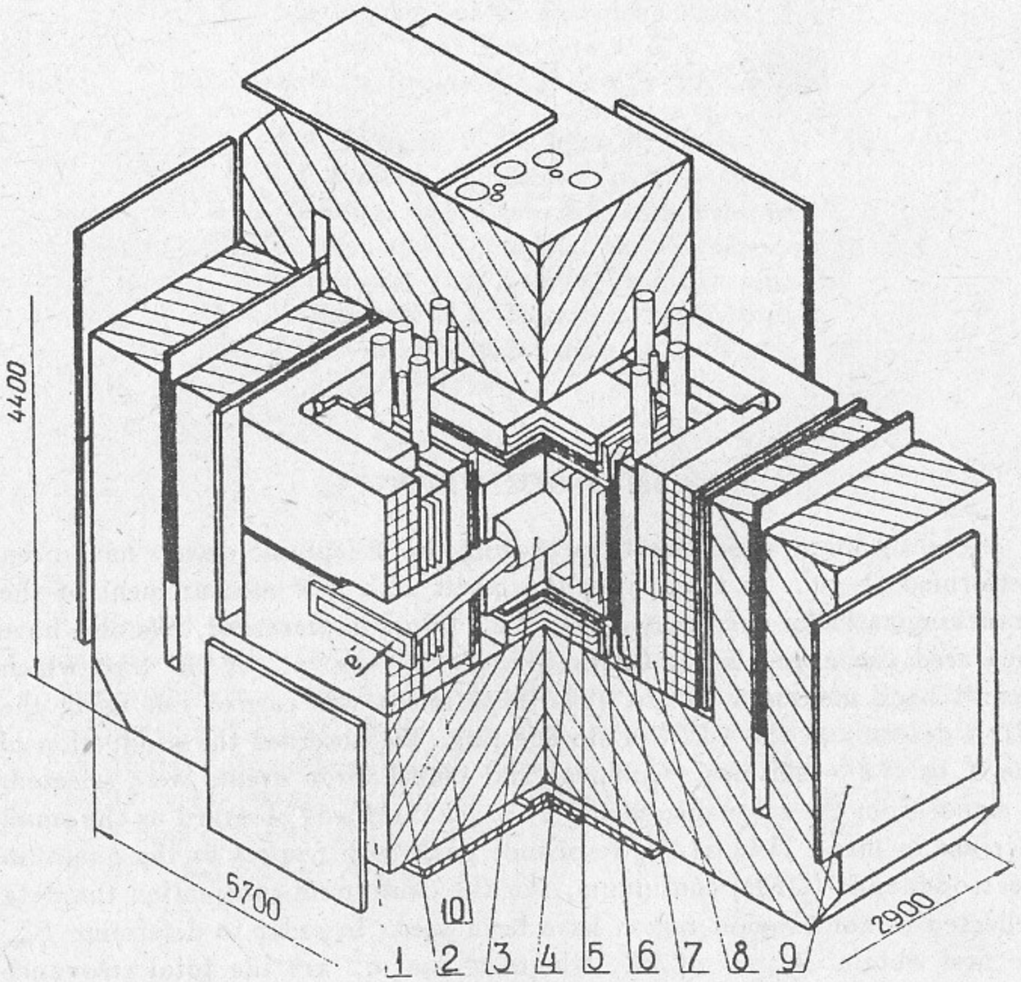


*Fig. 1.* The layout of the MD-1 detector. *1*–magnet yoke, *2*–magnet winding, *3*–vacuum chamber, *4, 8, 10*–shower-range chambers, *5*–scintillation counters, *6*–coordinate chambers, *7*–gaseous Cherenkov counters, *9*–muon chambers.

The particle momentum measurements are performed in a solid angle of $0.4 \times 4\pi$ sr with the resolution $\sigma_p/P = (5 \div 7\%) \cdot p$, where $p$ is in GeV/c. The coordinate system is surrounded by 24 scintillation counters (SC) placed at the sides of cube. Four counters have been mounted at the each side. The scintillation counters provide the time-of-flight resolution $\sigma_{\text{tof}} = 1.1$ ns (rms) and cover 90% of the total solid angle. Photons and electrons are detected in the shower-range proportional chambers which consist of 14 separate units. Each unit contains 10 chambers alternating with 13 mm thick stainless steel plates. The chamber wires are joined in the strips with a 4–10 cm width. The



adjacent chambers measure two orthogonal coordinates. For the energy loss measurement the amplitude of each chamber is used. A solid angle covered by the shower-range chambers is of $0.8 \times 4\pi$ sr. All these elements of MD-1 are placed in the transverse magnetic field.

The muon system consists of 48 units with dimensions $65 \times 1.36$ m. Each unit contains two proportional chambers which measure two orthogonal coordinates with an accuracy $\sim 25$ mm (rms). The muon chambers are placed behind the coil ($t \sim 420$ g/cm$^2$ inside the yoke ($t \sim$750 g/cm$^2$), and behind the yoke ($t \sim$1000 g/cm$^2$)). The muon system covers $\sim 60\%$ of the total solid angle.

The calibrations of the storage ring energy were carried out by the method of resonance depolarization [11, 12]. The synchrotron radiation photons scattered by the oppositely moving beam were used to control the beam polarization [13].

Two types of the trigger logic ($T_1$, $T_2$) were used during the experiment and two different data sets have been taken. In the trigger firing of at least one scintillation counter and two proportional chambers ($T_1$) or two shower-range units ($T_2$) situated on both sides from the beam axis are required. For the $T_2$ trigger at least two chambers in one unit which measure different coordinates must have fired. The trigger efficiency for the QED process $e^+e^- \to \mu^+\mu^-$ is 35.7% and 44.9% for $T_1$ and $T_2$ respectively.

A more detailed description of the MD-1 detector can be found elsewhere [14, 15].

## 2. EVENT SELECTION AND THE MAIN BACKGROUND PROCESSES

The collinear events were selected in two stages. The first one consists of soft cuts to obtain the low multiplicity events. At least 2 and no more than 4 scintillation counters are required. Only events with one or two clusters in the shower-range units are used for the following analysis. The total number of the chambers in one cluster must be more than 4 and at least 2 chambers in each projection are demanded.

The particle tracks were not reconstructed separately. Because of the collinearity of the $\mu^+\mu^-$ events, the common track was reconstructed. For noncollinear events the missing chambers appear, i.e. the chambers where the track intersection point is situated far from the hit ($> 50$ mm). In order to select the collinear events the number of the missing chambers ($N_m$) must be less than 9. If 2 or more adjacent chambers are missed the condition $N_m < 5$ is required.

These requirements effectively remove the events from the reactions $e^+e^-$-hadrons, $e^+e^- \to \tau^+\tau^-$ and $e^+e^- \to e^+e^-\mu^+\mu^-$. Using Monte-Carlo simulation we estimate the background contribution of 0.5, 0.6 and 3.2% respectively. The contributions of all the background processes in this section are given compared to the QED process $e^+e^- \to \mu^+\mu^-$ at $\sqrt{s} = 9.6$ GeV.

At the second stage more detailed cuts are applied to reject cosmic ray (CR) and Bhabha events. Muon time of arrival and tracking information gives the following criteria to remove the CR background.

1. The minimum distance ($R_v$) from the track to the beam axis must be less than 16 mm and 32 mm for $\theta > 45^o$ and $\theta < 45^o$ respectively, where $\theta$ is the angle between the beam axis and the track.

2. The event origin along the beam direction must be within $\pm 4 \cdot \sigma_x$ of the interaction point, where $\sigma_x$ is the longitudinal rms spread of the luminous region.

3. The average time of the scintillation counters ($T_i$) must be within $\pm 2 \cdot \sigma_{\rm tof}$ of the bunch crossing time.

4. The time of flight ($T_f$) must be within the interval [–4. ns, $T_c$], where $T_c$ is the parameter of the cut (Fig. 2). After all the cuts the cosmic ray contamination of about 5% is remained. The cosmic ray events rejected by cut 3 were used to find the CR background. The loss of the $\mu^+\mu^-$ events due to cut 4 was determined using the left slope of the time-of-flight distribution ($T_f < T_c$). In order to estimate the systematic error the dependence of the corrected number of $\mu^+\mu^-$-pairs on the cut parameter $T_c$ was examined (Tab. 1). The correction accounts for the cosmic ray background and the loss of the $\mu^+\mu^-$ events.

Table 1.

The Corrected Number of $\mu^+\mu^-$ Pairs

| $T_c$, ns | The $\mu$-pair loss % | CR background % | The number of $\mu^+\mu^-$-pairs |
|---|---|---|---|
| 1.56 | $7.9 \pm 0.3$ | $2.6 \pm 0.2$ | 9660 |
| 2.12 | $3.2 \pm 0.2$ | $3.4 \pm 0.3$ | 9669 |
| 2.69 | $1.2 \pm 0.2$ | $4.9 \pm 0.4$ | 9672 |

The result doesn't depend on the cut parameter and we estimate the systematic error due to the cosmic ray subtraction to be less than 0.5%.

Because of the transverse magnetic field in the detector the electrons from the single bremsstrahlung process (SB) give the accidental coincidences with



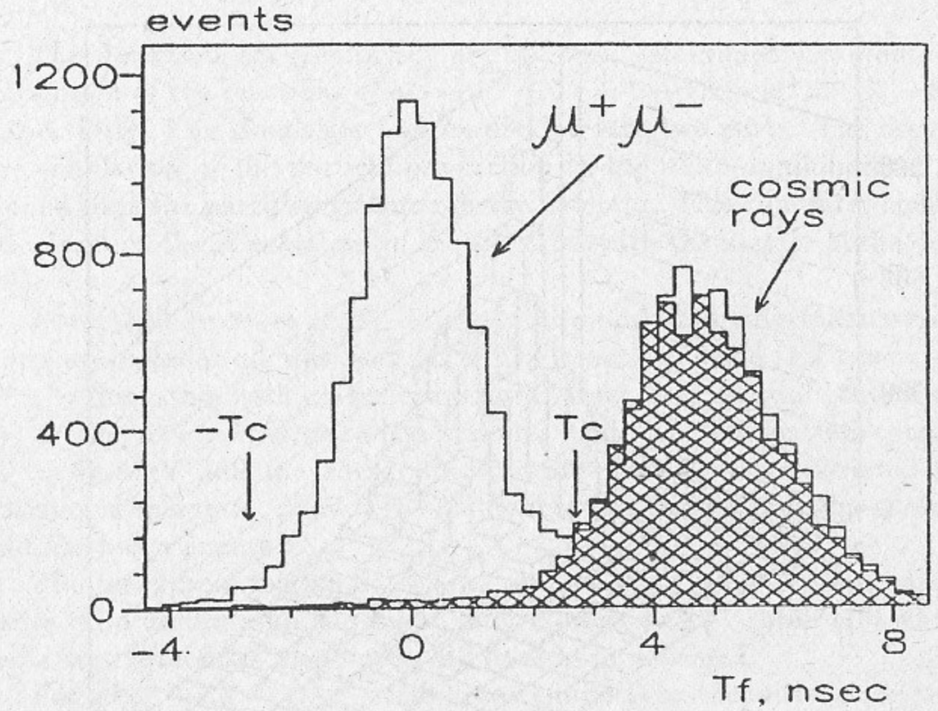


*Fig. 2.* The time of flight distribution for two data samples: $\square$ – $2 \cdot \sigma_{\rm tof} < T_i < 2 \cdot \sigma_{\rm tof}$; $\boxtimes$ – $T_i < -2 \cdot \sigma_{\rm tof}$ and $T_i > 2 \cdot \sigma_{\rm tof}$.

cosmic rays. The count rate of the SC system due to the SB process was $30 \div 40$ kHz. When a cosmic muon and a SB electron pass through the same scintillation counter, with the muon coming later, the time of the counter is naturally in coincidence with the bunch crossing time. The measured contamination by these events is $0.7 \pm 0.2\%$ and this result is in a good agreement with calculation ($0.5 \pm 0.2\%$).

The following cuts were used to remove the Bhabha events.

5. The average energy deposition ($E_c$) per shower-range chamber must be less than 5 keV. To improve the $e-\mu$ separation we excluded about $40 \div 50\%$ of the chambers with minimum and maximum amplitudes and the remaining chambers were used to calculate $E_c$. For muons the $E_c$ distribution has a close to Gaussian shape with mean 2.4 keV and rms deviation 0.5 keV.

6. For $e^+e^-$ events the hits in the shower-range chambers are wide, i.e. one hit consists of the several wire's groups. Often two and more hits in one chamber are appeared. For $\mu^+\mu^-$ events the chambers mainly have single-group hits, and the additional hits are usually absent. In Fig. 3 the two-dimensional plot for muons and Bhabha events is shown. The number of

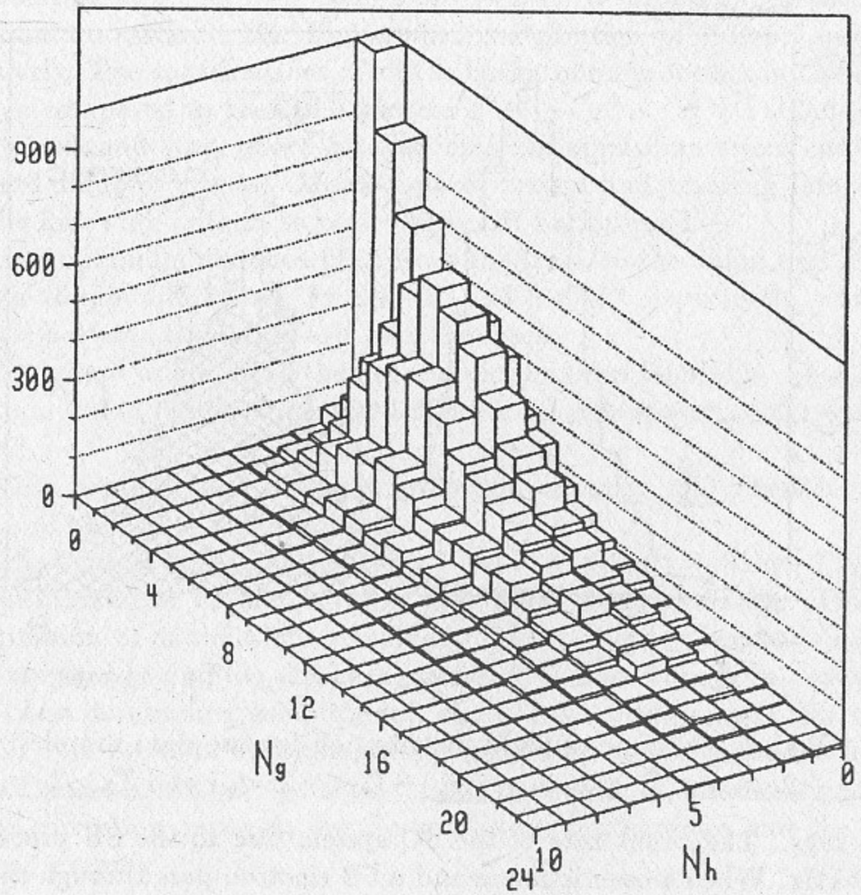


*Fig. 3.* The two-dimensional distribution over the $N_g$ and $N_h$.

the additional groups $N_g$ and additional hits $N_h$ are on the axes. The events are classified as background if $N_g > 9$ or if $N_g > 3$ and $N_h > 0$.

7. The energy deposition in each scintillation counter must be less than 12 MeV. It's possible to use the SC amplitudes for $e$-$\mu$ separation because $1.7X_0$ of material is before the counters. Since there is no correlation between the two SC amplitudes, the Bhabha contamination could be determined.

The contributions of the main background processes are shown in Tab. 4.

The hadron events were selected using the momenta of the particles and the multiplicity. We classified the events as multihadron if a) more than 3 charged and neutral particles were detected, b) the sum of the momenta ($\mid \Sigma\vec{p}_i \mid$) more than $300 \div 700$ MeV (depends on the charge multiplicity), c) the sum of the momentum projections at the beam axis was less than $2/3 \cdot \mid \Sigma\vec{p}_i \mid$ (to suppress two-photon background).



## 3. SIMULATION

The detection efficiencies $\varepsilon_c^\mu$, $\varepsilon_r^\mu$, $\varepsilon_r^h$ were determined by Monte Carlo simulation of the reactions $e^+e^- \to \mu^+\mu^-$, $e^+e^- \to \Upsilon \to \mu^+\mu^-$, $\Upsilon \to$hadron respectively. The simulation can be divided into two parts. The first one is the simulation of the particle production in the $e^+e^-$-annihilation. In the second part the particles go through the detector. This computer code takes into account the interactions of the particles with the matter of the detector [16].

For QED process $e^+e^- \to \mu^+\mu^-$ the simulation with radiative corrections up to order $\alpha^3$ was used [17]. The computer code [18] generated the $\mu^+\mu^-\gamma$ final state with a photon energy $k$ larger than a certain cut-off energy $k_1$, or the $\mu^+\mu^-$ final state if $k$ was less than $k_1$. The cut-off energy was $k_1 = 50$ MeV and the energy of the hard photons was restricted by the maximum energy $k_m = E \cdot (1 - \xi^2)$, where $\xi$ is the ratio of the muon mass and the beam energy $E$.

The total cross section $\sigma_q$ for the process $e^+e^- \to \mu^+\mu^-$ was calculated using the formula from the paper of E. Kuraev and V. Fadin [19] where the radiative corrections up to order $\alpha^4$ have been obtained.

For $e^+e^- \to \Upsilon \to \mu^+\mu^-$ the photon emission by the initial state particles is suppressed. Therefore the detection efficiency $\varepsilon_r^\mu$ was obtained from the same simulation as for $e^+e^- \to \mu^+\mu^-$ but with the photon emission in the final state only.

The efficiencies of the chambers and counters were determined with the cosmic rays during the experiment and were used in the simulation.

The trigger and detection efficiencies for two types of the trigger are shown in Tab. 2. In the last column the result of the simulation without radiative corrections is shown. The first error is the simulation statistic uncertainty and the second error is defined by the efficiency uncertainty of the chambers and counters.

Table 2.

**The Trigger ($\varepsilon_t$) and Detection ($\varepsilon_d$) Efficiencies**

| Data set | % | $e^+e^- \to \mu^+\mu^-$ | $\Upsilon \to \mu^+\mu^-$ | Without RC |
|---|---|---|---|---|
| $T_1$ | $\varepsilon_t$ | $35.7 \pm 0.3 \pm 0.4$ | $40.9 \pm 0.8 \pm 0.4$ | $41.6 \pm 0.9 \pm 0.4$ |
| | $\varepsilon_d$ | $23.2 \pm 0.3 \pm 0.3$ | $32.9 \pm 0.8 \pm 0.4$ | $35.6 \pm 0.9 \pm 0.4$ |
| $T_2$ | $\varepsilon_t$ | $44.9 \pm 0.4 \pm 0.2$ | $51.4 \pm 0.8 \pm 0.2$ | $52.2 \pm 0.9 \pm 0.2$ |
| | $\varepsilon_d$ | $29.2 \pm 0.3 \pm 0.2$ | $41.4 \pm 0.8 \pm 0.2$ | $44.7 \pm 0.9 \pm 0.2$ |

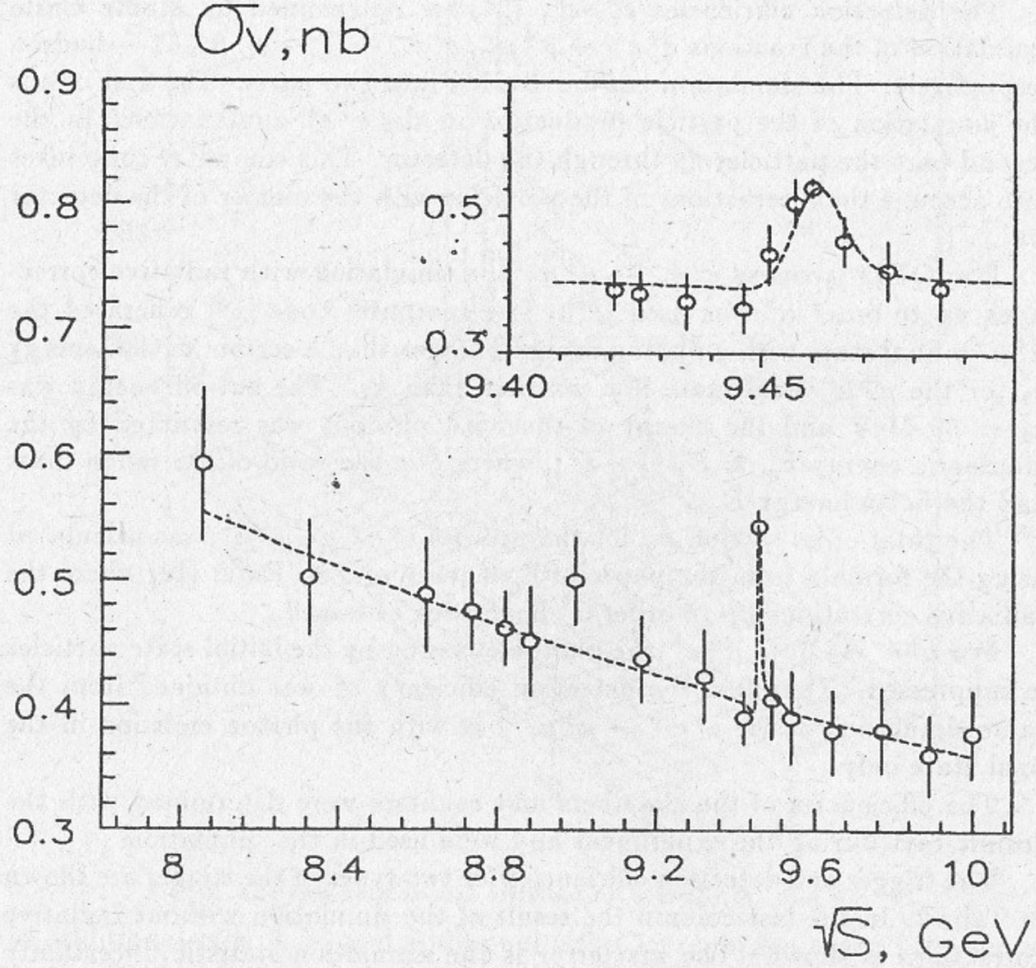


*Fig. 4.*. The visible cross section $e^+e^- \to \mu^+\mu^-$.

The simulation of the hadronic decays of the $\Upsilon$ was carried out with LUND6.3 computer code. The detection efficiency $\varepsilon_\tau^h$ was obtained to be $87 \pm 2\%$. The contamination of the decays $\Upsilon \to \tau^+\tau^-$ was estimated to be 0.3%.

## 4. MEASUREMENT OF THE QED CROSS SECTION

Our event selection resulted in the visible cross section $\sigma_v(s)$ of Fig. 4. The fitting of the experimental data (excluding the resonance region) was carried out with one free parameter: the continuum cross section $\sigma_{vc}^o$ at



$\sqrt{s} = 9.46$ GeV. In Tab. 3 the results of the fit for different energy intervals are shown.

Table 3.

**The Continuum Cross Section $\sigma_{vc}^o$ for Different Energy Intervals**

| Run | Trigger | $\sqrt{s}$, GeV | $\sigma_{vc}^0$, nb |
|---|---|---|---|
| 1 | $T_1$ | $9.42 \div 9.50$ | $0.331 \pm 0.027$ |
| | $T_2$ | $9.42 \div 9.50$ | $0.384 \pm 0.015$ |
| 2 | $T_2$ | $8.00 \div 8.66$ | $0.404 \pm 0.020$ |
| | | $8.66 \div 8.86$ | $0.392 \pm 0.012$ |
| | | $8.86 \div 9.43$ | $0.413 \pm 0.012$ |
| | | $9.43 \div 0.02$ | $0.397 \pm 0.010$ |

Taking into account the detection efficiency (Tab. 2) and combining all $\sigma_{vc}^o$ measurements one obtains the total cross section for the reaction $e^+e^- \to \mu^+\mu^-$ at the continuum

$$\sigma_c = 1.362 \pm 0.018 \pm 0.035 \text{ nb}.$$

The systematic error accounts for uncertainties in the detection efficiency (1.2%), background subtraction (Tab. 4), and absolute luminosity calibration (2.1%). The measured cross section is in a good agreement with theoretical calculation $\sigma_q = 1.404$ nb.

Table 4.

**The Background and Systematic Errors**

| The source of background | Background % | Systematic error, % |
|---|---|---|
| cosmic rays | 4.9 | 0.5 |
| $e^+e^- \to e^+e^-$ | 2.1 | 0.4 |
| CR and SB coincidence | 0.7 | 0.3 |
| $e^+e^- \to$hadron (simul.) | 0.6 | 0.2 |
| $e^+e^- \to \tau^+\tau^-$ (simul.) | 0.4 | 0.4 |
| $e^+e^- \to e^+e^-\mu^+\mu^-$ (simul.) | 3.2 | 0.7 |
| sum | 11.9 | 1.1 |

The results of the luminosity calibration that have been used in the $B_{\mu\mu}$ measurement (section 5) are given below.

For the luminosity measurements mainly the elastic $e^+e^-$-scattering at small angles (SA monitor) was used [20]. In Tab. 5 the results of the monitor calibration that was carried out with the processes double bremsstrahlung (DB), Bhabha scattering at large angles (LA, $\theta > 45^o$), and $e+e^- \to \mu^+\mu^-$ (MM) are shown. It contains also the result of relative calibration for two runs using Bhabha scattering at middle angles (MA, $12^o < \theta < 45^o$). The detection cross section $\sigma_{SA}$ of the SA monitor is different for the first and second runs. This difference is associated with the modification of the SA monitor in the shutdown between the runs.

Table 5.

The Results of the SA Monitor Calibration

| Method | Run | $\sigma_{SA} \times 10^{29}$ cm$^2$, $\sqrt{S} = 9.46$ GeV | $\sigma^1_{SA}/\sigma^2_{SA} - 1$, % |
|---|---|---|---|
| DB | 1 | $3.58 \pm 0.05 \pm 0.06$ | |
| LA | 1 | $3.75 \pm 0.07 \pm 0.04$ $\pm 0.06$ | $6.8 \pm 3.3$ |
| | 2 | $3.51 \pm 0.08 \pm 0.04$ | |
| MM | 1 | $3.88 \pm 0.13$ $\pm 0.05$ | $8.9 \pm 3.6$ |
| | 2 | $3.56 \pm 0.05$ | |
| MA | | — | $6.0 \pm 1.8$ |

## 5. $B_{\mu\mu}$ MEASUREMENT

The lowest order cross section for reaction $e^+e^- \to \mu^+\mu^-$ incorporating a resonance with mass $M$, total width $\Gamma_{tot}$ and leptonic width $\Gamma_{ee}$ reads [21]

$$\sigma_t(s) = \frac{4\pi\alpha^2}{3s}\,(1 + 2\cdot \mathrm{Re}\{B(s)\} + \mid B(s) \mid^2), \qquad (2)$$

$$B(s) = \frac{\beta \cdot s}{s - M^2 + i\cdot\Gamma_{tot}\cdot N}; \qquad \beta = \frac{3\cdot\Gamma_{ee}}{\alpha\cdot M}.$$

The three terms in Eq. 2 give the QED ($\sigma_o$), the interference ($\sigma_I$) and the resonance ($\sigma_R$) cross section. The experimental cross section is quite different from the cross section $\sigma_t$ because the machine energy has certain width $\sigma_w$ and also the energy of the initial state electrons is degraded by the bremsstrahlung emission [22, 23]. The muon cross section was approximated by the following formula



$$\sigma^\mu_v = \sigma^\mu_c(w) + \sigma^\mu_r \epsilon^\mu_r \sigma_\mu(w)/\sigma_\mu(M), \qquad (3)$$

where $w$ is the center of mass energy.

Two parameters were free: the observed cross section at the continuum $\sigma^\mu_c(M)$ and the resonance's excess above the continuum $\sigma^\mu_r$. The ratio $\sigma_\mu(w)/\sigma_\mu(M)$ that gives the shape of the resonance curve was calculated by the formulas

$$\sigma_\mu(w) = \int_0^\infty dw'' F(w,w'')[\sigma_R(w'') + \sigma_I(w'')](1. + \delta_a) = \sigma_r(w) + \sigma_i(w),$$

$$F(w,.w'') = \frac{1}{\sigma_w}\left(\frac{2\sigma_w}{W}\right)^t \frac{\Gamma(1+t)}{\sqrt{2\pi}} \exp{-\frac{x^2}{4}}\, D_{-t}(-x), \qquad (4)$$

$$x = \frac{(w - w'')}{\sigma_w}; \quad t = \frac{2\alpha}{\pi}\left(2\ln\left(\frac{w}{m_e}\right) - 1\right); \quad \delta_a = \frac{\alpha}{\pi}\left(\frac{\pi^2}{3} - \frac{1}{2}\right) + \frac{3}{4}t.$$

where $m_e$ is the electron mass, $\alpha$ is the fine structure constant, $\Gamma(1+t)$ is a gamma-function, $D_{-t}(-x)$ is a Weber's parabolic cylinder function. The hadron cross section was approximated by the same way as the muon cross section (Eq. 3)

$$\sigma^h_v(w) = \sigma^h_c(w) + \sigma^h_r \epsilon^h_r \sigma_r(w)/\sigma_r(M).$$

The continuum and resonance interference for multihadron events is negligible and the shape of the hadronic resonance curve was calculated without the interference term in Eq. 4. The results of the data analysis are summarized in Tab. 6, where the $\sigma^\mu_r$ and $\sigma^h_r$ cross sections, the measured number of

Table 6.

The Resonance Cross Sections for Hadrons and Muons, $N_{\mu\mu}$, $\bar{B}_{\mu\mu}$ for Two Different Data Sets $T_1$ and $T_2$

| | $\sigma^h_r$, nb | $\sigma^\mu_r$, nb | $N\mu\mu$ | $\bar{B}_{\mu\mu}$, % |
|---|---|---|---|---|
| $T_1$ | $15.8 \pm 0.13$ | $0.348 \pm 0.045$ | $276 \pm 36$ | $2.20 \pm 0.28$ |
| $T_2$ | $15.4 \pm 0.14$ | $0.357 \pm 0.042$ | $339 \pm 40$ | $2.32 \pm 0.27$ |

$\mu$-pairs from the resonance decays ($N_{\mu\mu}$), and $\bar{B}_{\mu\mu}$ are shown. The errors are statistical and were obtained by the fitting with fixed value of the continuum $\sigma_c^\mu$.

Using Eq. 1 and adding the statistical error due to the continuum subtraction we obtain the branching ratio: $B_{\mu\mu} = 2.12 \pm 0.20\%$.

The systematic error for the branching ratio $B_{\mu\mu}$ is determined by the accuracy of detection efficiencies $\varepsilon_\tau^\mu$ (2.2%), $\varepsilon_\tau^h$ (2.0%), and by the following three effects: a) the luminosity instability, b) the storage ring energy instability, c) the background from the $\Upsilon$ decays into hadrons. All these effects are described below.

The main data at the continuum were taken in the second run. In order to use it for the continuum subtraction, the cross section in the second run was scaled by $\sigma_{SA}^1/\sigma_{SA}^2$. This ratio was obtained using LA and MA monitors (Tab. 5) and the final systematic error was estimated to be 3.2%.

The ratio of the muon and hadron yields from the $\Upsilon$ decays gives the branching ratio $B_{\mu\mu}$ when the center-of-mass energy $w$ is equal to the resonance mass $M$ (without radiative correction). If $w$ is not equal $M$, the interference between resonance and continuum should be taken into account. In Fig.5

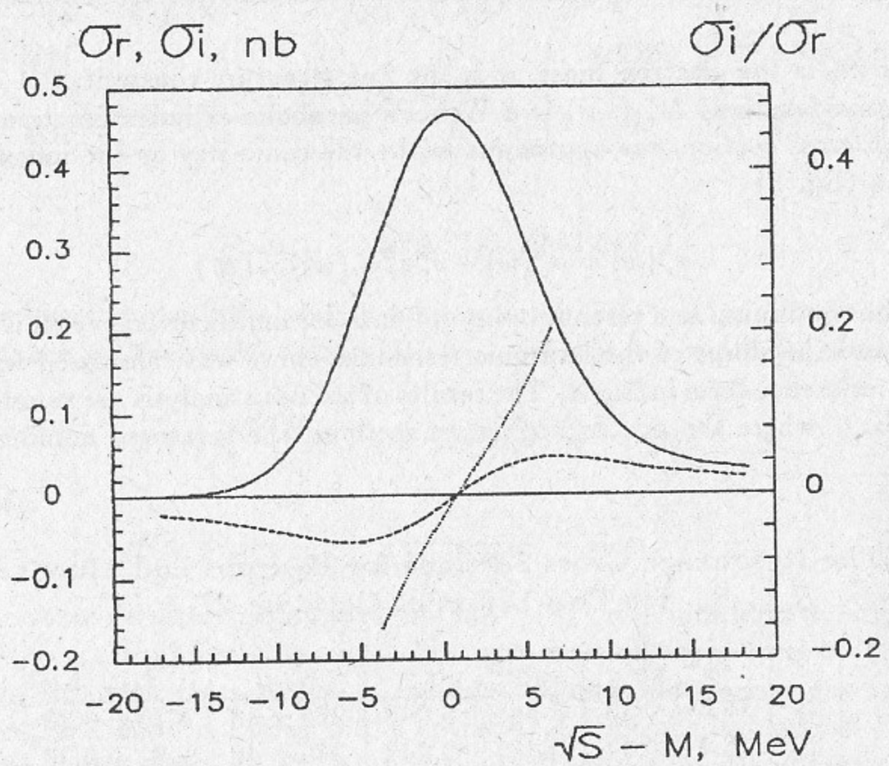


*Fig. 5.* The calculated cross sections $\sigma_\tau$ (—), $\sigma_i$ (- - -), and the ratio $\sigma_i/\sigma_\tau$ (···).



the calculated cross sections $\sigma_i$, $\sigma_r$, and their ratio are shown. In the calculation the leptonic width $\Gamma_{ee} = 1.34$ keV and the VEPP-4 energy spread $\sigma_w = 4.62$ MeV were used. Ratio $\sigma_i/\sigma_r$ gives the alteration of the $B_{\mu\mu}$ value dependent on the center-of-mass energy if the interference is omitted:

$$\frac{dB_{\mu\mu}}{dw} = \frac{d}{dw}(\sigma_i/\sigma_r) = 3.25\%/\text{MeV}.$$

Usually, the energy of the beams is obtained from the magnetic field value in one of the storage ring magnets. This energy ($w_m$) may be different from the real energy ($w_r$) by a few MeV. On the other hand the changes in the storage ring regime and the temperature instability of the ring geometry result in the instability of the $w_m$ value. The results of the energy calibrations which were performed with the method of resonance depolarization are shown in Fig.6.

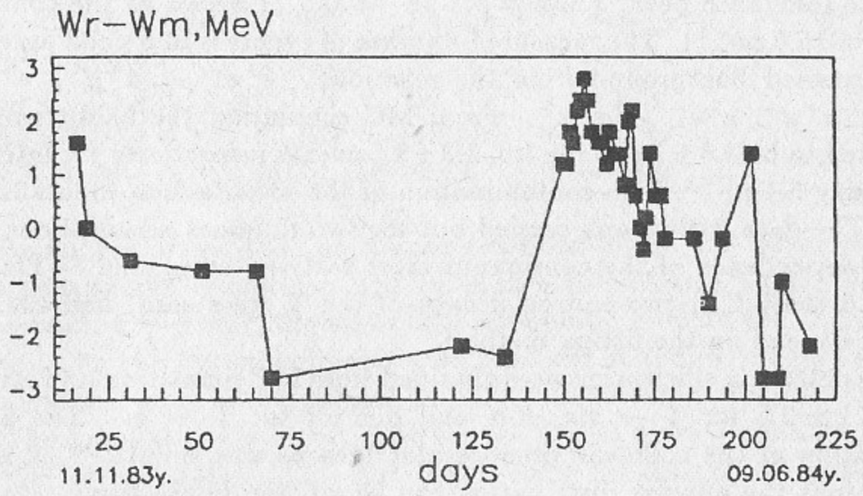


*Fig. 6.* The results of the storage ring energy calibration.

The connection of the $w_m$ value with the real energy $w_r$ was taken from two nearby calibrations. The systematic error for $B_{\mu\mu}$ associated with the uncertainty of the beam energy is 0.8%.

The contamination of the $\Upsilon$ hadron decays was determined from the simulation and it was estimated to be 1.2%±0.7%.

Finally, the probability of the reaction $\Upsilon \to \mu^+\mu^-$ is

$$B_{\mu\mu} = (2.12 \pm 0.20 \pm 0.10)\,\%.$$

## SEARCH FOR DECAYS $\Upsilon \to \pi^+\pi^-$, $K^+K$, $p\bar{p}$

For the upper limits measurement the collinear events with $\theta > 45^o$ were used. The $\mu$-pairs rejection have been performed using the muon chambers. The chamber firing was checked if the reconstructed track pass through the muon chamber. The particles were classified as muons if at least one chamber inside the yoke or behind the yoke was fired. If muons weren't revealed, the events where the number of the track's intersections with more than 1 nonfiring chambers were selected. To reduce the background from the reaction $e^+e^- \to e^+e^-\mu^+\mu^-$ the additional selection conditions on the vertex parameter $R_v$ and the maximum momentum of the particles $P$ were imposed: $R_v < 10$ mm and $P > 2$ GeV. If the particles momentum wasn't measured the cut was $R_v < 5$ mm. There wasn't any hadron identification.

Finally, we have obtained 5 events in the resonance (in the interval $\pm\sigma_w$ near the resonance peak, $\int Ldt = 5.1$ pb$^{-1}$) and 21 events at the continuum ($\int Ldt = 15.0$ pb$^{-1}$). The measured number of events is in a good agreement with expected background from the reactions $e^+e^- \to \mu^+\mu^-$, $e^+e^- \to$ $\to e^+e^-\mu^+\mu^-$, $e^+e^- \to e^+e^-$. From MC simulation the background was estimated to be $2.5\pm1.0$, $3.0\pm3.0$, $2.3\pm1.5$ events respectively for integrated luminosity 5.1 pb$^{-1}$. The contamination of the multihadron events is negligible. The data fitting was carried out for two different assumptions about energy dependence of the continuum cross section: const and $\sim 1/s$. Less than 4.3 (90% CL) two-hadron decays of the $\Upsilon$ were seen, and the result doesn't depend on the fitting method.

The detection efficiencies were obtained from MC simulation and estimated to be $11 \pm 2\%$ for $\Upsilon \to \pi\pi$, $KK$ and $6 \pm 1\%$ for $\Upsilon \to p\bar{p}$. The angular distribution of the collinear pseudoscalar mesons was simulated as $\sin^2(\theta)$. For protons the angular distribution can be written in the form: $d\sigma/d\Omega \sim$ $\sim 1 + \alpha \cdot \cos^2(\theta)$. We put $\alpha = 1.0$, that is close to the calculation [24]: $\alpha \simeq 0.92$.

Finally, the upper limits on branching ratio for the decays $\Upsilon \to \pi^+\pi^-+$ $+K^+K^-$ and $\Upsilon \to p\bar{p}$ is $5 \cdot 10^{-4}$ and $9 \cdot 10^{-4}$ respectively (90% CL). Theoretical estimations give essentially less branching ratios. For example, the calculation with QCD sum rules [25] gives the following branching ratios: $B_{\pi\pi} \sim 5 \cdot 10^{-8}$, $B_{KK} \sim 10^{-7}$, $B_{p\bar{p}} \sim 10^{-7}$.

## CONCLUSIONS

The result obtained with the MD-1 detector for the branching ratio of the decay $\Upsilon \to \mu^+\mu^-$ agrees with the results of the previous experiments (Tab. 7).



Table 7.

**The Branching Ratio for the Decay $\Upsilon \to \mu^+\mu_-$ Obtained in Different Experiments**

| $B_{\mu\mu}$, % | Experiment | Reaction |
|---|---|---|
| $2.2 \pm 2.0$ | PLUTO [1], 79 | $\Upsilon \to \mu^+\mu^-$ |
| $1.4^{+3.4}_{-1.4}$ | DESY-HD [2], 80 | $\Upsilon \to \mu^+\mu^-$ |
| $3.8 \pm 1.5 \pm 0.2$ | LENA [3], 82 | $\Upsilon \to \mu^+\mu^-$ |
| $3.2 \pm 1.3 \pm 0.3$ | DASP [4], 82 | $\Upsilon \to \mu^+\mu^-$ |
| $2.7 \pm 0.3 \pm 0.3$ | CLEO [5], 83 | $\Upsilon \to \mu^+\mu^-$ |
| $2.70 \pm 0.28 \pm 0.14$ | CUSB [6], 83 | $\Upsilon \to \mu^+\mu^-$ |
| $2.84 \pm 0.18 \pm 0.20$ | CLEO [7], 84 | $\Upsilon' \to \pi^+\pi^-\Upsilon$; $\Upsilon \to \mu^+\mu^-$ |
| $2.30 \pm 0.25 \pm 0.13$ | ARGUS [8], 87 | $\Upsilon' \to \pi^+\pi^-\Upsilon$; $\Upsilon \to \mu^+\mu^-$ |
| $2.61 \pm 0.09 \pm 0.11$ | CUSB [9], 89 | $\Upsilon \to \mu^+\mu^-$ |
| $2.52 \pm 0.07 \pm 0.07$ | CLEO [10], 89 | $\Upsilon \to \mu^+\mu^-$ |
| $2.12 \pm 0.20 \pm 0.10$ | MD-1 this exp. | $\Upsilon \to \mu^+\mu^-$ |

It should be noted, that an absolute calibration of the beam energy is necessary and the continuum and resonance interference should be taken into account. Otherwise, the additional systematic error in the $B_{\mu\mu}$ value is possible. The two last experiments with the least statistical errors have been carried out using the CUSB [9] and CLEO [10] detectors at the CESR storage ring. The calculated value $dB_{\mu\mu}/dw$ for the CESR energy spread $\sigma_w = 3.23$ MeV [26] is 4.5%/MeV. The systematic error because of the interference wasn't discussed in above mentioned papers.

For the first time the upper limits on the branching ratio for the decays $\Upsilon \to \pi^+\pi^-$, $K^+K^-$, $p\bar{p}$ have been obtained. The experimental results are substantially larger (of $3 \div 4$ orders) than theoretical predictions.

We wish to thank the VEPP-4 and MD-1 operating staff for their assistance during experiment. We also wish to thank E.Kuraev and V.Fadin who participated in discussion concerning the radiative corrections.

*REFERENCES*

1. *Ch. Berger et al.* Z. Phys., C1 (1979) 343.

2. *P. Rock et al.* Z. Phys., C6 (1980) 125.

3. *B. Niczyporuk et al.* Z. Phys., C15 (1982) 299.

4. *H. Albrecht et al.* Phys. Lett., 116B (1982) 383.

5. *P.M. Tuts.* Cornell conf., (1983) 284.

6. *D. Andrews et al.* Phys. Rev., Lett. 50 (1983) 807.

7. *D. Besson et al.* Phys. Rev., D30 (1984) 1433.

8. *H. Albrecht et al.* Z. Phys., C35 (1987) 283.

9. *W.-Y. Chen et al.* Phys. Rev., D39 (1989) 3528.

10. *T.M. Kaarsberg et al.* Phys. Rev. Lett., 62 (1989) 2077.

11. *S.I. Serednyakov.* Zh. Eksp. Teor. Fiz., 71 (1976) 2026.

12. *Ya.S. Derbenev.* Particle accelerators, 10 (1980) 177.

13. *A.E. Blinov et al.* Nucl. Inst. Meth., A241 (1985) 80.

14. *S.E. Baru et al.* Proc. of the III Intern. Conf. on Instrum. for Colliding Beam Physics. Novosibirsk, (1984) 262.

15. *A.E. Blinov et al.* Z. Phys., C48 (1990) 581.

16. *A.D. Bukin et al.* Novosibirsk, Preprint INP 84-33 (1984).

17. *F.A. Berends, R. Kleiss.* Nucl. Phys., B177 (1981) 237;
*F.A. Berends, R.Kleiss, S. Jadach.* Nucl. Phys., B202 (1982) 63.

18. *F.A. Berends, R.Kleiss, S.Jadach.* Comp. Phys. Comm., 29 (1983) 185.

19. *E.A. Kuraev, V.S. Fadin.* Sov. Jour. Nucl. Phys., 41 (1985) 466.

20. *A.E. Blinov et al.* Nucl. Inst. Meth., A273 (1988) 31.

21. *F.A. Berends, R. Kleiss.* Nucl. Phys., B115 (1976) 114.

22. *Y.S. Tsai..* SLAC-PUB-1515, Dec.7, 1974.

23. *J.D. Jackson, D.L. Scharre.* Nucl. Inst. Meth., 128 (1975) 13.

24. *M. Claudson et al.* Phys. Rev., D25 (1982) 1345.

25. *V.L. Chernyak, A.R. Zhitnitsky.* Phys. Reports, 112 (1984) 175.

26. *W.W. MacKay et al.* Phys. Rev., D29 (1984) 2483.



*S.E. Baru, M.V. Beilin, A.E. Blinov,*
*V.E. Blinov, A.E. Bondar, A.D. Bukin,*
*V.R. Groshev, S.G. Klimenko, G.M. Kolachev,*
*A.P. Onuchin, V.S. Panin, I.Ya. Protopopov,*
*A.G. Shamov, V.A. Sidorov, Yu.I. Skovpen,*
*A.N. Skrinsky, V.A. Tayursky, V.I. Telnov,*
*Yu.A. Tikhonov, G.M. Tumaikin, A.E. Undrus,*
*A.I. Vorobiov, V.N. Zilich*

**Measurement of the Branching Ratio for $\Upsilon(1S)$ State into $\mu^+\mu^-$ and Search for Decays $\Upsilon(1S) \to \pi^+\pi^-$, $K^+K^-$, $p\bar{p}$**

*С.Е. Бару, М.В. Бейлин, А.Е. Блинов,*
*В.Е. Блинов, А.Е. Бондарь, А.Д. Букин,*
*В.Р. Грошев, С.Г. Клименко, Г.М. Колачев,*
*А.П. Онучин, В.С. Панин, И.Я. Протопопов,*
*А.Г. Шамов, В.А. Сидоров, Ю.И. Сковпень,*
*А.Н. Скринский, В.А. Таюрский, В.И. Тельнов,*
*Ю.А. Тихонов, Г.М. Тумайкин, А.Е. Ундрус,*
*А.И. Воробьев, В.Н. Жилич*

**Измерение относительной вероятности распада $\Upsilon(1S)$ состояния в $\mu^+\mu^-$ и поиск распадов $\Upsilon(1S) \to \pi^+\pi^-$, $K^+K^-$, $p\bar{p}$**

Ответственный за выпуск С.Г. Попов

Работа поступила 25 октября 1991 г.
Подписано в печать 25.02 1992 г.
Формат бумаги 60×90 1/16 Объем 1,3 печ.л., 1,0 уч.-изд.л.
Тираж 220 экз. Бесплатно. Заказ N 110

Обработано на IBM PC и отпечатано на
ротапринте ИЯФ им Г.И. Будкера СО РАН,
*Новосибирск, 630090, пр. академика Лаврентьева, 11.*